Near-infrared spectral signatures differentiate blue stain and brown rot fungi in conifer and broadleaf trees

*Emmanuel A. Boakye**
Natural Resources Canada
Canadian Forest Service, Edmonton, AB T6H-3S5, Canada
emmanuel.boakye@nrcan-rncan.gc.ca / eaaboakye@yahoo.com

*Jennifer Klutsch**
Natural Resources Canada
Canadian Forest Service, Edmonton, AB T6H-3S5, Canada
jennifer.klutsch@nrcan-rncan.gc.ca

Cyriac S. Mvolo
Natural Resources Canada
Canadian Forest Service, Edmonton, AB T6H-3S5, Canada
cyriac.mvolo@nrcan-rncan.gc.ca

Andre G. Duarte
Natural Resources Canada
Canadian Forest Service, Edmonton, AB T6H-3S5, Canada
andregalvd@gmail.com

(Received 30 May 2025)

Abstract. Colonization by blue stain and brown rot fungi affects timber quality in distinct ways. Blue stain fungi cause discoloration without reducing wood properties, while brown rot fungi degrade wood tissues, resulting in brittleness and brown coloration. Given these chemical differences, we investigated whether near-infrared spectroscopy (NIRS) could distinguish between these fungal types. We hypothesized that early fungal attack would produce unique spectral signatures, allowing for rapid identification. Wood disc samples were collected from white spruce, lodgepole pine, and trembling aspen in Fox Creek, northwest Alberta, Canada, ca. 4 months after a wildfire. The trees were colonized by fungi associated with blue and brown sapwood discoloration and analyzed using NIRS. In white spruce, we found consistent and significant absorbance differences between blue- and brown-discolored sapwood across each 100 nm segment. In lodgepole pine, the most distinct differences occurred in the 1650–1750 nm, 2050–2150 nm, and 2350–2450 nm ranges. For trembling aspen, differences were evident across most 100 nm intervals, except 2150–2250 nm. Permutational multivariate analysis of variance (PERMANOVA) indicated greater spectral dissimilarity between fungal types in white spruce and trembling aspen, with less pronounced differences in lodgepole pine. Our findings suggest that NIRS can effectively classify fungal-discolored wood in white spruce and trembling aspen within the first year following wildfire. However, its application to lodgepole pine in the same timeframe may be less reliable.

Keywords: Fungal colonization; Blue stain fungi; Brown rot fungi; Wood discoloration; Near-infrared spectroscopy (NIRS); Spectral signatures

Introduction

Canada's boreal forest plays a vital role in domestic and international wood markets, contributing 1.2% to the national GDP in 2022 and accounting for 12% of global wood supply (Natural Resources Canada 2022, 2023). However, threats like fires, pests, and diseases threaten the forest health and wood quality (Gauthier et al. 2015). From 1984 to 2016, wildfires and insect outbreaks caused 53.7% of forest biomass loss, surpassing the 43.8% from industry harvesting (Wulder et al. 2020). In 2023, wildfires burned over twice the previous record area of 6.7 million hectares set in 1989 (Jain et al. 2024). Between 1998 and 2009, insects like the mountain pine beetle killed an estimated 675 million m³ of pine in Western Canada (Natural Resources Canada 2020). With temperatures projected to rise between 2°C and 6°C by the end of the century, increasing fire and pest activity could threaten the forests' economic viability (Natural Resources Canada 2019).

Wildfires significantly impact timber value, as burned trees may become unsuitable for commercial use, and salvaged

* Corresponding author

wood often has lower product value (Watson and Potter 2004; Bousfield et al. 2023). The heat from wildfires triggers pyrolysis, a chemical decomposition that alters the wood's structure and composition, reducing moisture content, darkening coloration, decreasing mechanical strength, and increasing brittleness (Mensah et al. 2023). These changes make the wood prone to cracking and degrade key mechanical properties, such as tensile strength and bending strength, rendering it unsuitable for structural applications (González-Peña et al. 2009; Piernik et al. 2022). Additionally, fire-damaged trees can become vulnerable to fungal, bacterial, and insect attack, which accelerates decay and further reduces the wood's commercial value.

Fungal growth in burnt wood is favored by conditions such as mild temperatures, moderate to low moisture levels, and increased aeration as the wood dries (Schmidt 2006; McCarthy et al. 2012). The fungal colonization in sapwood is distinguished by patterns like blue and brown discoloration. Blue stain fungi, generally from the class Ascomycota, do not degrade lignin or cellulose (McCarthy et al. 2012; Lundell et al. 2014). Instead, they invade living wood and produce melanin to protect themselves from environmental stressors, breaking down non-structural components like triglycerides and oleic acid. This activity results in discoloration appearing as shades of blue but causes minimal structural damage (Lundell et al. 2014). In contrast, fungi that cause brown rot are typically associated with the class Basidiomycota and often cause severe damage that degrades cellulose (McCarthy et al. 2012; Lundell et al. 2014). This leaves behind a brown rot characterized by brittle, cracked residues composed mainly of lignin that significantly compromises the wood's structural integrity (McCarthy et al. 2012; Lundell et al. 2014). Both blue stain and brown rot fungi reduce the cosmetic quality of timber, but brown rot fungi also render it unsuitable for structural use (McCarthy et al. 2012).

Given the potential for widespread fungal damage in burnt wood, tools that quickly and accurately assess wood properties and the presence of fungal-caused discolouration are essential for early intervention to minimize damage (Pohleven et al. 2002; Guillén and Machuca 2008). In this regard, near-infrared spectroscopy (NIRS) can be an efficient tool for analyzing these characteristics. By utilizing the near-infrared (NIR) region of the electromagnetic spectrum (700 to 2500 nm), NIRS measures how electromagnetic energy is scattered or absorbed by wood tissues, providing understanding into their composition and quality (Tsuchikawa and Kobori 2015). The light interacts with the overtone and combination vibrations of chemical bonds (e.g., C-H, O-H, N-H) within organic compounds, producing NIRS spectra that can be analyzed to obtain information about the chemical properties of organic materials (Chen et al. 2015; Tsuchikawa and Kobori 2015). This technique is valuable for forest management because it offers rapid data acquisition, high accuracy, and requires minimal sample preparation, making it ideal for large-scale studies (Tsuchikawa 2007; Tsuchikawa and Kobori 2015; Hein et al. 2017).

NIRS is particularly useful for analyzing wood composition and assessing quality changes due to fungal damage. Previous studies demonstrated that NIRS can capture molecular-level alterations in wood coloration from fungal activity. Via et al. (2007) observed distinct absorbance shifts due to blue stain in longleaf pine; Kelley et al. (2002) and Barton et al. (1995) detected lignin and carbohydrate degradation from white and brown rot fungi; and Fackler et al. (2007) and Fackler and Schwanninger (2012) monitored decay progression and mass loss. Building on this, Burud et al. (2014) used hyperspectral NIRS imaging to quantify blue stain in Norway spruce. Unlike visual inspection, which detects only advanced discoloration, NIRS provides an accurate alternative, identifying early-stage and subsurface decay in wood that may not be identified by visual methods. By detecting chemical changes such as lignin or cellulose degradation, NIRS enables fungal damage detection before visible signs emerge, thus representing a more refined and precise method in wood quality assessment (Pohleven et al. 2002; Guillén and Machuca 2008).

This study builds on previous research by using NIR spectroscopy to assess the effects of blue stain and brown rot fungi on NIR absorbance in two coniferous and a deciduous tree species, focusing on white spruce (*Picea glauca* (Moench) Voss), lodgepole pine (*Pinus contorta* Douglas ex Loudon), and trembling aspen (*Populus tremuloides* Michx.). Since fungal infestations alter organic chemical bonds in wood, we aimed to determine whether colonization influenced NIR absorbance in species-specific ways, as NIR is sensitive to molecular vibrations of organic compounds (Tsuchikawa and Kobori 2015; Deepa et al. 2024). We expected that differences in how blue stain and brown rot fungi interact with sapwood would allow for the differentiation of their spectral characteristics. To this end, we hypothesized that the unique chemical and physical alterations caused by each fungal type would manifest in distinct spectral patterns, enabling reliable wood quality assessment. This is the first step in evaluating the potential of NIR as a tool for understanding the role of fungi in wood degradation in fire-killed trees. Based on these results, future work will aim to identify fungi species associated with these stains and further clarify their contribution to wood decay.

Materials and methods

Wood samples

In 2023, a forest inventory was conducted in the native forests near Fox Creek, Alberta (54.476°N, 116.783°W), to assess the impact of fire on wood quality. This area has a history of periodic disturbances, primarily wildfire, that shape the composition and structure of its boreal forests. During the inventory, some harvested trees were found to be infested with fungi. The sampled tree species included white spruce (average age based on ring counts = 88 years), lodgepole pine (average age = 77 years), and trembling aspen (average age = 73 years), all of which are common in Alberta's boreal forests. Discs from the infested trees were collected at a height of 2 m from the base to ensure consistency in wood properties. The wood exhibited minimum degradation but advanced discoloration (Figure 1). The presence of fungi associated with blue stain and brown rot (Table 1) was confirmed by the Mycology Research Laboratory of the Canadian Forest Service in Edmonton, Canada.

Acquisition of spectra in the NIR region

Spectral readings were collected from the flat transverse surface of the wood sample discs. For each disc, five scan locations were selected per observed type (e.g., blue stain or brown rot) to capture variation across the visibly stained regions (Table 1), along with five additional scans from clear areas confirmed as unstained by visual inspection. In cases where multiple stain types were present on a single disc, five scans were taken for each type. Control discs taken from trees with no visible staining were scanned at five locations across the clear surface.

Clear scans from visibly unstained areas on stained discs enabled direct comparisons of near-infrared spectral characteristics within a consistent tree-specific context. Control scans from entirely unstained discs of the same species served as a baseline reference free of fungal influence.

To ensure uniform surface conditions, the samples were lightly pre-sanded to remove chainsaw marks that could interfere with spectral readings. Sanding was applied consistently across each sample. Measurements were conducted at room temperature (approximately 22°C) to control for environmental effects on the readings and were performed using a single NeoSpectra-Scanner (Si-Ware Systems Inc., USA). The device features a 10-mm collection window, and its software reports spectra from 1350 to 2550 nm at a step of 2.5 nm, with a wavelength resolution of 16 nm. The scanner lens was positioned on the dried wood surface and held steady during each scan to minimize interference from ambient light. At each measurement location, three spectra were collected and averaged to reduce noise.

Table 1. Summary of data samples showing the number of trees and total scans per species under four wood conditions. Total scans refer to the number of measurements taken on wood discs from each species under each condition. Control refers to scans from completely unstained discs collected from healthy trees of the same species. Clear refers to scans from visibly unstained areas on otherwise stained discs.

Wood condition	Species	Number of trees	Total scans
Blue stain fungi	Lodgepole pine	5	25
	Trembling aspen	3	15
	White spruce	6	30
Brown rot fungi	Lodgepole pine	3	15
	Trembling aspen	5	27
	White spruce	3	15
Clear	Lodgepole pine	6	30
	Trembling aspen	6	30
	White spruce	7	35
Control	Lodgepole pine	5	25
	Trembling aspen	5	25
	White spruce	5	25

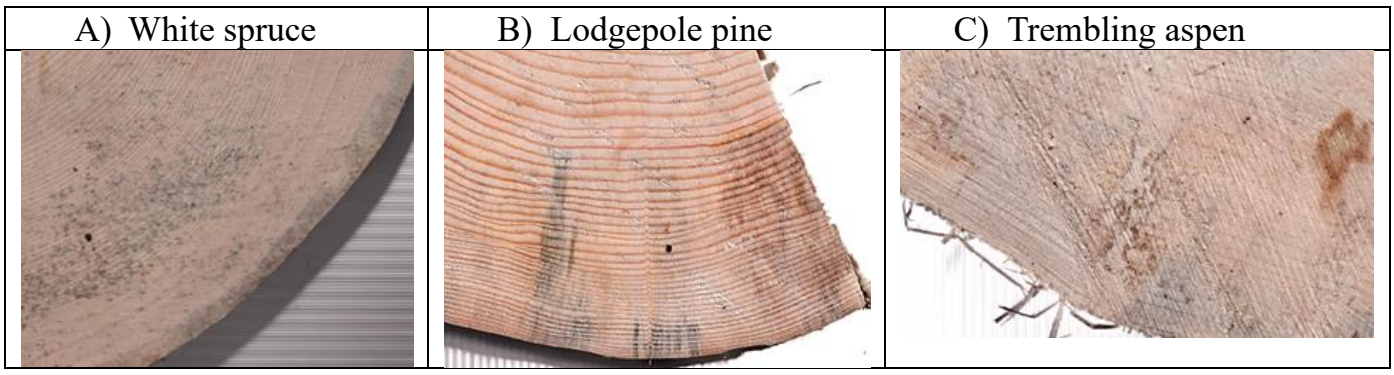

Figure 1. Cross-section segments of white spruce, lodgepole pine, and trembling aspen showing brownish and bluish stains on the wood surface.

Spectral pre-processing

Near-infrared spectroscopy data pose challenges due to broad, overlapping absorption bands that can shift depending on physical, chemical, and structural factors. These shifts and overlaps can obscure the resolution of spectral features and make direct interpretation difficult. To address these issues, derivatives are commonly used for baseline correction in spectroscopy (Savitzky and Golay 1964). The first derivative removes additive shifts, while the second eliminates linear increases and sharpens peaks. The application of these derivatives also enhances resolution, resolves overlapping peaks, and highlights spectral details.

With these considerations, two pre-processing techniques were applied to enhance spectral features and reduce noise:

1. No pre-treatment: Using raw or original absorbance values.
2. Savitzky-Golay smoothing with first- and second-order derivatives: This method, proposed by Savitzky and Golay (1964), was implemented with a window size of 13 data points and a polynomial order of 2. These parameters were selected based on exploratory analysis and their effectiveness in resolving overlapping peaks and correcting baselines, as demonstrated in previous studies (e.g., Via et al. 2007).

The signal package (signal developers, 2023) in R software (R Core Team 2024) was used for the Savitzky-Golay filtering of the spectral data.

Data Analysis

Spectral data were analyzed to identify regions with absorbance peaks and assess differences in mean absorbance across four wood conditions: clear wood, blue-stained wood, brown rot wood, and control samples. The spectral range was divided into 100-nm segments to capture localized variations in absorbance, and the average absorbance within each segment was compared across the wood conditions. A Kruskal-Wallis test was applied to each segment, followed by Dunn's post-hoc test to determine specific differences between the wood conditions. A permutational multivariate analysis of variance (PERMANOVA) was conducted on similarity matrices based on Euclidean distances using the *vegan* package in R (Oksanen et al. 2024). PERMANOVA was chosen because it evaluates for differences among groups in multivariate space without assuming normality. This analysis assessed whether the centroids representing each wood condition were significantly different, indicating variation in spectral patterns across treatments. To mitigate the risk of too few unique permutations, the Monte Carlo method was used to obtain reliable p-value estimates. If PERMANOVA indicated significant differences among the wood conditions, pairwise comparisons were performed to assess the statistical significance of the Euclidean distances between the wood condition centroids.

Results and discussion

Spectral properties of stained and unstained wood across species

We observed variations in the spectral properties (Figure 2) of white spruce, lodgepole pine, and trembling aspen across four conditions: blue stain fungi, brown rot fungi, clear wood, and control wood. In white spruce (Figure 2A), brown rot fungi exhibited the highest absorbance across most wavelengths, especially around 1450 nm, 1900 nm, and 2350 nm. Blue stain fungi followed closely with slightly lower absorbance, while the control and clear wood conditions showed lower values, with clear wood consistently having the lowest absorbance overall. Additionally, significant differences in mean absorbance between the blue stain and brown rot fungi were consistently observed at 100-nm intervals along the spectral curve.

In the 1st derivative plot of white spruce (Figure 2A), the spectral curves across conditions were generally similar, though some differences appeared around 1550 nm and 2150 nm, where the brown rot showed slightly higher peaks. The control, brown rot, and blue stain fungi curves overlapped closely, while the clear condition displayed a slightly different pattern, particularly around 1750 nm and 2350 nm. In the 2nd derivative plot, minor variations emerged between the conditions. The blue stain, brown rot, and control conditions deviated more visibly from the clear wood, especially between 1750 nm and 1950 nm, and at 2350 nm, where their patterns were distinct. Additionally, no significant differences in mean absorbance were detected between the blue and brown rot fungi for both the first and second derivatives at 100-nm intervals along the spectral curve.

For lodgepole pine (Figure 2B), the patterns were similar, with blue stain fungi showing the highest overall absorbance, particularly between 1900 and 2350 nm. Brown rot fungi and clear wood exhibited moderate absorbance, with brown rot fungi slightly higher than clear wood across most wavelengths, while the control had the lowest absorbance. The peak around 1900 nm was especially pronounced in the blue stain fungi sample. Additionally, significant differences in mean absorbance between blue and brown rot fungi were consistently observed at 100-nm intervals along the spectral curve.

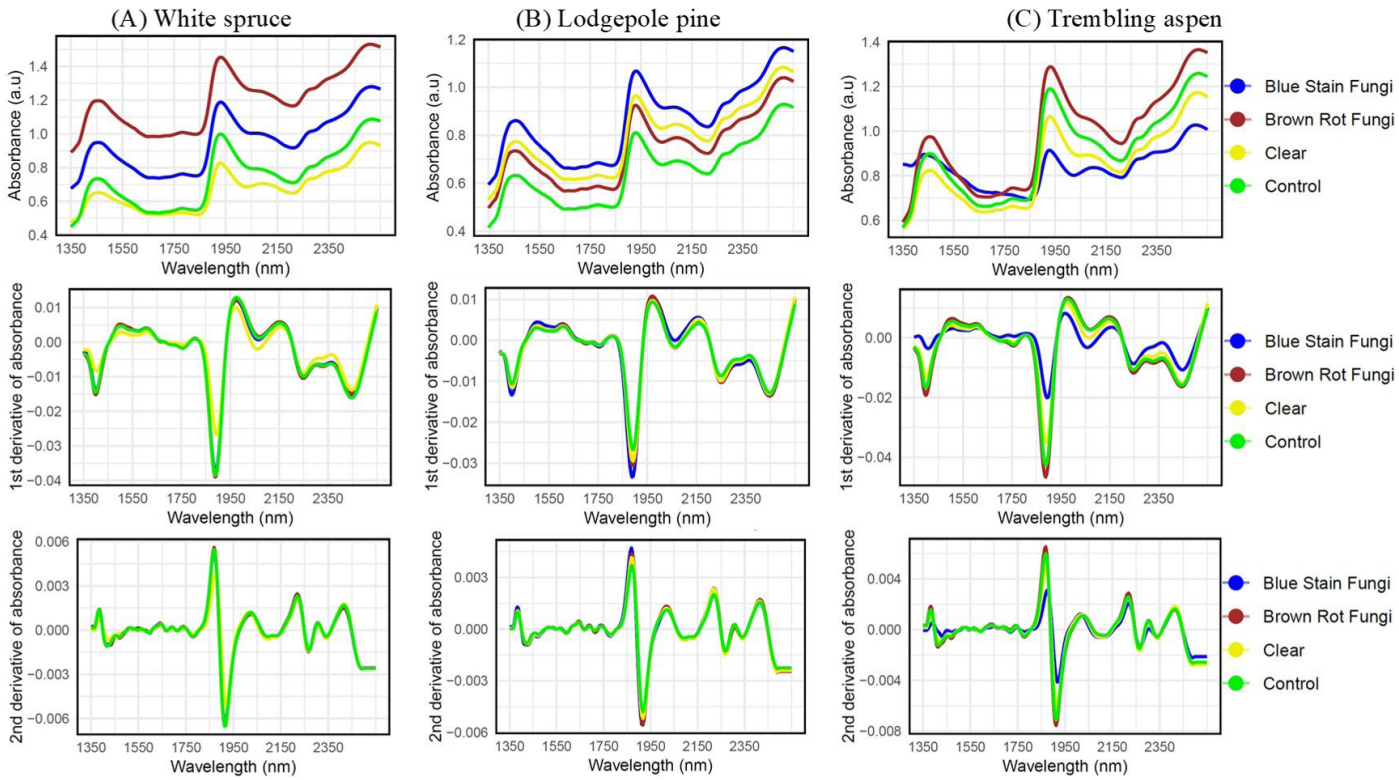

Figure 2. Average absorbance (top row), first derivative ($dA \cdot dw^{-1}$, middle row), and second derivative ($d^2A \cdot dw^{-2}$, bottom row) spectra as functions of wavelength (1350–2450 nm) for each species. The four wood conditions are color-coded: blue stain fungi (blue), brown rot fungi (brown), clear wood (yellow), and control (green). Each curve represents the mean spectrum for its respective condition.

In the first derivative curves of lodgepole pine (Figure 2B), there was a clearer distinction between blue stain fungi and brown rot fungi, especially around 1950 nm. Clear wood and the control overlapped significantly across most regions, with minimal variation between them, particularly in the 1550–1950 nm range. Significant differences in mean absorbance between the blue and brown rot fungi were observed in the wavelength intervals of 1650–1750 nm, 2050–2150 nm, and 2350–2450 nm.

The second derivative curves (Figure 2B) showed similar trends. The blue and brown rot fungi samples displayed distinct patterns around 1950 nm, while clear wood and the control remained closely aligned throughout the spectrum, with minor variation between them. Significant differences in mean absorbance between the blue and brown rot fungi were evident in the intervals of 1650–1750 nm, 1950–2050 nm, and 2050–2150 nm.

For trembling aspen (Figure 2C), the brown rot fungi showed the highest absorbance, particularly between 1750 and 2350 nm, with distinct peaks around 1900 nm and 2350 nm. Control and clear wood followed similar patterns but exhibited lower absorbance compared to the brown rot fungi. In contrast, the blue stain fungi consistently displayed the lowest absorbance across the wavelength range. At 100-nm intervals along the spectral curve, significant differences in mean absorbance were observed between the blue and brown rot fungi at most wavelengths, except for the intervals 1450–1550, 1550–1650, 1650–1750, and 1750–1850.

In the first derivative of trembling aspen (Figure 2C), differences were more pronounced around 1950 nm, where the brown rot fungi separated more clearly from the other spectra. The curves for clear wood and control samples largely overlapped across most regions, while the blue stain fungi showed some separation around 1850 nm. Additionally, at 100-nm intervals, significant differences in mean absorbance were consistently detected between the blue and brown rot fungi, except in the 2150–2250 nm range.

In the second derivative (Figure 2C), the brown and blue stain fungi exhibited sharper peaks around 1850 nm and 1950 nm, whereas the clear wood and control curves remained closely aligned, showing minimal variation in these regions. Again, significant differences in mean absorbance were observed at 100-nm intervals between the blue and brown rot fungi,

except for the intervals 1350–1450, 1750–1850, 1950–2050, 2250–2350, and 2350–2450 nm.

Our results demonstrate that NIRS can distinguish between brown rot and blue stain fungi in white spruce, lodgepole pine, and trembling aspen, based on distinct spectral signatures (Figure 2, Table 2) that reflect underlying chemical and physical changes. The variations in absorbance with wavelength, particularly at 1900 nm, 1950 nm, and 2350 nm, emerged as consistent markers for distinguishing blue stain and brown rot fungi across all three species (Figure 2). These wavelengths were reliable indicators due to their consistent presence in multiple spectral analyses (raw, 1st derivative, and 2nd derivative) across species. Specifically, the 1900 nm and 1950 nm regions are sensitive to water and hydroxyl (-OH) groups associated with cellulose and water molecules (Via et al. 2008;

Table 2. PERMANOVA and pairwise comparisons of wood stained/rot or unstained by fungi. F represents the F-statistic, and p represents the p-value from PERMANOVA. Significant at p value less than 0.05. A dash indicates that the overall PERMANOVA was not significant enough to warrant pairwise comparisons.

A. White spruce						
Source/Comparison	F	p	F	p	F	p
	Raw Absorbance		1st Derivative		2nd Derivative	
Overall PERMANOVA	31.647	0.001	9.589	0.001	9.396	0.001
Pairwise comparison						
Control vs. brown rot fungi	52.408	0.001	0.19	0.711	0.203	0.757
Control vs. clear	4.342	0.032	26.817	0.001	25.43	0.001
Control vs. blue stain fungi	18.003	0.002	0.293	0.562	0.239	0.692
Brown rot fungi vs. clear	77.166	0.001	22.452	0.001	20.633	0.001
Brown rot fungi vs. blue stain fungi	10.442	0.006	0.224	0.664	0.204	0.78
Clear vs. blue stain fungi	40.142	0.001	20.64	0.001	21.756	0.001
B. Lodgepole pine						
Source/Comparison	F	p	F	p	F	p
	Raw Absorbance		1st Derivative		2nd Derivative	
Overall PERMANOVA	4.763	0.006	1.341	0.256	1.469	0.214
Pairwise comparison						
Control vs. blue stain fungi	14.676	0.001	-	-	-	-
Control vs. brown rot fungi	5.57	0.019	-	-	-	-
Control vs. clear	6.508	0.011	-	-	-	-
Blue stain fungi vs. brown rot fungi	2.842	0.097	-	-	-	-
Blue stain fungi vs. clear	1.251	0.277	-	-	-	-
Brown rot fungi vs. clear	0.447	0.503	-	-	-	-
C. Trembling aspen						
Source/Comparison	F	p	F	p	F	p
	Raw Absorbance		1st Derivative		2nd Derivative	
Overall PERMANOVA	2.0674	0.102	14.056	0.001	11.269	0.001
Pairwise comparison						
Control vs. brown rot fungi	-	-	1.693	0.161	1.505	0.205
Control vs. clear	-	-	4.265	0.038	4.304	0.034
Control vs. blue stain fungi	-	-	29.252	0.001	23.936	0.001
Brown rot fungi vs. clear	-	-	11.724	0.001	10.121	0.004
Brown rot fungi vs. blue stain fungi	-	-	50.507	0.001	34.153	0.001
Clear vs. blue stain fungi	-	-	12.119	0.002	8.729	0.002

Sundaram et al. 2015). Blue stain fungi alter water distribution and cellulose structure, leading to significant absorption differences at these wavelengths. Similarly, the 2350 nm region is linked to lignin, which contains aromatic structures and fewer hydroxyl groups (Belt et al. 2022; Fackler and Schwanninger 2012). Unlike lignin-degrading fungi, brown rot fungi do not significantly alter lignin, and the resulting spectral consistency at this wavelength emphasizes the importance of their minimal impact on this component, aiding in their differentiation.

Our findings also highlight tree species-specific differences in the wavelengths that distinguish blue stain and brown rot fungi (Figure 2). For white spruce, subtle but visible distinctions appeared in the raw spectral curve around 1450 nm, 1900 nm, and 2350 nm, where brown rot fungi exhibited higher absorbance, likely due to chemical changes caused by fungal activity. Additional observations in the derivative plots, such as around 1550 nm and 2150 nm, provided further insights into spectral patterns. In lodgepole pine, blue stain fungi exhibited the highest absorbance in the raw curve between 1900–2350 nm, peaking around 1900 nm, suggesting links to fungal metabolite concentrations. Derivative plots further differentiated key intervals, including 1650–1750 nm, 1950–2150 nm, and 2350–2450 nm, emphasizing the utility of derivative analyses (Schwanninger et al. 2011). For trembling aspen, brown rot fungi showed dominant absorbance from 1750–2350 nm, particularly at 1900 nm and 2350 nm, while derivative plots revealed variability around 1850 nm and 1950 nm. These results demonstrate the potential of these wavelengths as reliable markers for species identification and wood quality assessment, aligning with findings from previous studies (Ramirez et al. 2015; Lang et al. 2017).

Multivariate analysis of NIR spectral differences among wood conditions and species

PERMANOVA and follow-up pairwise comparisons were used to assess the NIR spectral similarity among the different wood conditions: blue stain, brown rot, clear, and control for the species white spruce, lodgepole pine, and trembling aspen. Despite some overlap in the multivariate ordination plots, significant differences were detected among the four wood conditions based on the original (raw) absorbance values, as well as the first and second derivatives.

For white spruce, a significant difference was observed between the blue stain and brown rot fungi for the raw absorbance, whereas the first and second derivatives showed no significant difference between the two fungal groups (Table 2A, Figure 3A). Various degrees of significance were also noted between the clear/control and both the blue stain and brown rot conditions (Table 2A).

For lodgepole pine (Table 2B, Figure 3B), the raw absorbance values showed no significant difference between the blue stain and brown rot conditions. Unlike clear wood, there was a significant difference in absorbance values between the control and both the brown rot and blue stain fungi. For the first and second derivatives, the overall PERMANOVA was not significant, so no pairwise comparisons were conducted between the different wood conditions (Table 2B).

In the case of trembling aspen (Table 2C, Figure 3C), PERMANOVA showed no significant differences in absorbance values between the blue stain, brown rot fungi, and their clear and control wood counterparts. However, PERMANOVA for the first and second derivatives revealed significant differences between the brown rot and blue stain fungi conditions. Significant differences were predominantly recorded between the control and clear wood, each compared separately to the brown rot and blue stain conditions.

Our results revealed species-specific differences in the spectral properties and the relative utility of raw absorbance versus derivative data for differentiating fungal stains (Figure 3, Table 2). In white spruce, significant differences between blue stain and brown rot fungi were observed in the raw absorbance spectra, particularly when compared to the clear and control wood conditions. However, the first and second derivatives did not reveal significant differences between the two fungal discoloration types. This suggests that the spectral changes induced by blue stain and brown rot fungi in white spruce are more detectable in the raw spectra. The lack of differentiation in the derivative plots may be due to the tendency of derivative processing to emphasize subtle spectral features while reducing broader signals, which could obscure meaningful changes if the fungal-induced variations are not sharply defined. Additionally, the spectral sampling interval of the instrument and the use of 100-mm spatial increments may have contributed to signal averaging, further limiting the detection of localized fungal effects. Nevertheless, pronounced differences were observed between stained and unstained wood (both clear and control conditions), confirming that NIR spectroscopy was effective in detecting fungal degradation relative to unaffected wood (Via et al. 2008).

These species-specific differences in PERMANOVA outcomes likely reflected underlying biological and chemical processes. In white spruce, the consistent and pronounced spectral shifts across brown rot, blue stain, and unstained (clear and control)

wood suggest that fungal colonization leads to substantial and predictable chemical changes, which are readily captured by raw spectra. In contrast, lodgepole pine exhibited more subtle and overlapping spectral responses, indicating that fungal impact may be less chemically pronounced or more spatially variable, making detection less reliable. For trembling aspen, the blue stain spectrum appeared atypical compared to all other spectra, potentially due to pigment accumulation, unique host-fungus interactions, or sampling variation. This irregularity likely contributed to the lack of significant group separation in the raw data. However, applying derivative transformations helped reveal meaningful contrasts in aspen by removing baseline noise and highlighting finer spectral details. These findings emphasize that both species-specific wood chemistry and spectral preprocessing approaches influence the detectability of fungal degradation in NIR spectra.

The ability to detect spectral changes caused by blue stain and brown rot fungi depends on whether raw or derivative spectra are used (Figures 2 and 3, Table 2). Derivative transformations, like first or second derivatives, are often applied to spectroscopic data to enhance spectral features and elimi-

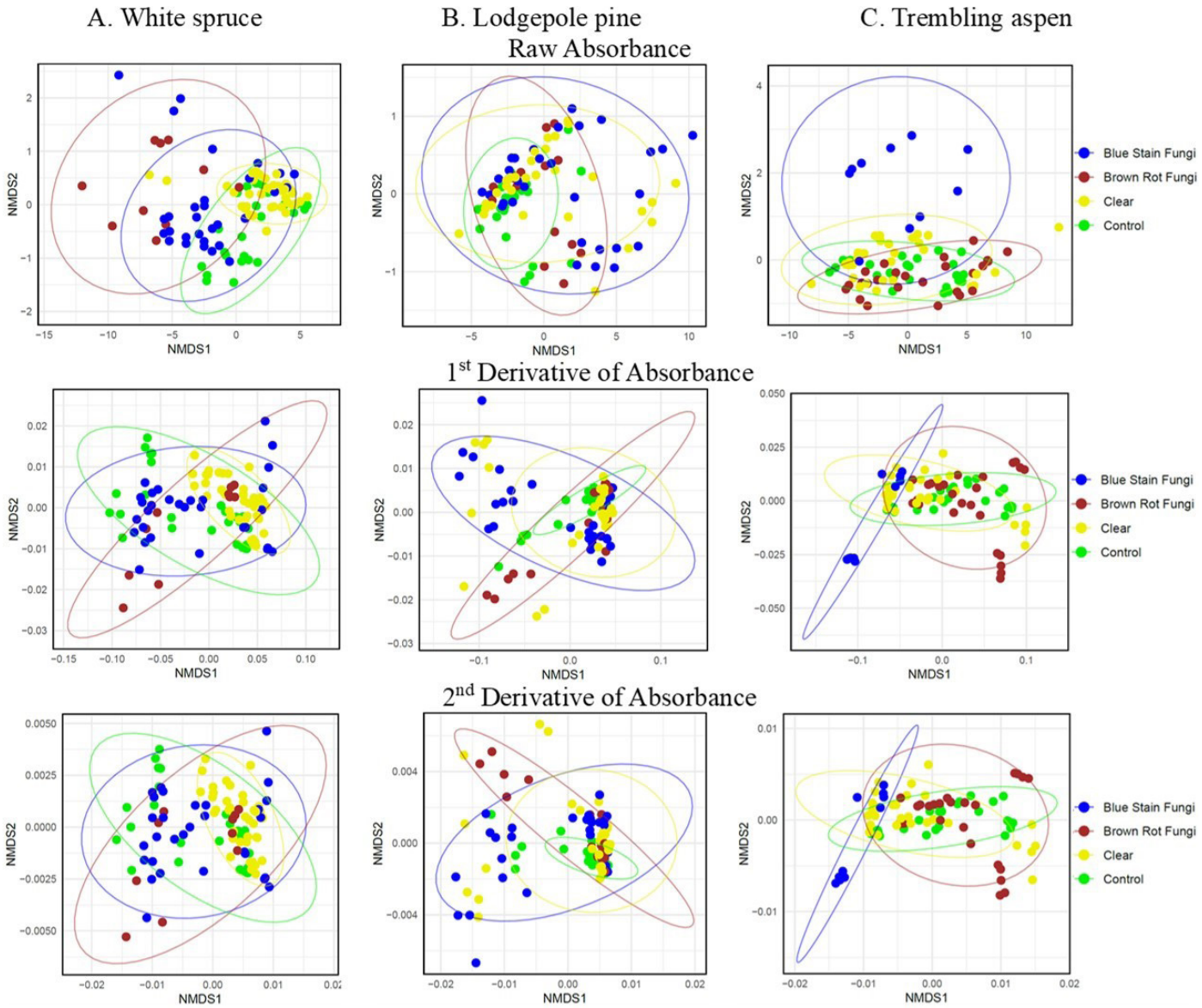

Figure 3. NMDS ordination from PERMANOVA showing spectral variability across four wood stain conditions in different tree species. Each column represents a species, and rows display raw absorbance (top), first derivative (middle), and second derivative (bottom). The four wood conditions: blue stain fungi (blue), brown rot fungi (brown), clear wood (yellow), and control (green) are represented using non-metric multidimensional scaling (NMDS) plots. Ellipses indicate the dispersion and overlap within each wood stain condition.

nate baseline variations. However, these transformations can sometimes reduce the ability to detect fungal-induced spectral changes due to increased noise. For example, Via et al. (2007 and 2008) identified significant differences in the raw spectra of longleaf pine affected by blue stain at specific wavelengths (e.g., 354–364 nm, 424–1104 nm, and 1114–1354 nm). These differences became less detectable after applying derivative transformations, highlighting that raw spectra alone can effectively identify fungal stains without requiring additional processing.

Regarding the observed significant differences between control and clear wood, although both were visually unstained, subtle chemical differences may exist due to residual microbial activity that could have influenced the clear samples prior to NIR measurement, making them spectrally distinct from the control set. This suggests that unstained regions on stained discs (clear wood) may not be chemically equivalent to wood from entirely non-colonized unstained trees (control), potentially reflecting early or localized biochemical alterations.

Conclusions

This study highlighted the potential of NIR spectroscopy to detect and differentiate fungal stains and rots in wood, with performance varying across tree species. In white spruce, raw absorbance spectra effectively distinguished stain from rot fungi. In trembling aspen, derivative analysis enhanced sensitivity to subtle spectral differences. However, in lodgepole pine, spectral overlap limited differentiation, suggesting a need for further exploration of the biochemical similarities among fungal types and the resulting wood degradation. These findings emphasize the importance of developing rapid, reliable methods for fungal identification, especially as climate-driven disturbances such as wildfires could alter the prevalence of fungal impacts on salvaged logs. Accurate detection can support informed forest management, efficient processing, and improved timber valuation.

Nonetheless, several factors limited the interpretation and generalizability of our results. Species-specific traits of trees such as age, size, site conditions, growth history, natural wood color, and durability, as well as sampling location, can influence spectral patterns. Moreover, because the samples were naturally stained in the field, we had no experimental control over fungal colonization or wood condition. While this enhanced ecological relevance, it necessitated caution in interpreting the results. These limitations were not directly evaluated in this study but should be systematically addressed in future research to strengthen model robustness and applicability. Moving forward, we plan to integrate genetic analyses to identify fungal species, explore the causes of staining, and clarify fungal functional roles. Combining NIR spectroscopy with complementary techniques will improve fungal discrimination and deepen understanding of the underlying spectral mechanisms.

Acknowledgment

The authors express their gratitude to the Canadian Wood Fibre Centre within Natural Resources Canada for providing financial support. We also extend our appreciation to the students who assisted with field data collection and sample processing for measurements. Additionally, we acknowledge the valuable comments provided by colleagues at the Canadian Wood Fibre Centre on the submitted manuscript.

References

Barton FE, Himmelsbach DS, Akin DE, Sethuraman A, Eriksson KE (1995) Two-dimensional vibrational spectroscopy III: interpretation of the degradation of plant cell walls by white rot fungi. J. Near Infrared Spectrosc, 3(1), 25-34.

Belt T, Awais M, Mäkelä M (2022) Chemical characterization and visualization of progressive brown rot decay of wood by near infrared imaging and multivariate analysis. Front Plant Sci 13:940745. https://doi.org/10.3389/fpls.2022.940745

Bousfield CG, Lindenmayer DB, Edwards DP (2023) Substantial and increasing global losses of timber-producing forest due to wildfires. Nat Geosci 16(12):1145-1150.

Burud I, Gobakken LR, Flø A, Kvaal K, Thiis TK (2014) Hyperspectral imaging of blue stain fungi on coated and uncoated wooden surfaces. Int Biodeterior Biodegrad 88, 37-43. https://doi.org/10.1016/j.ibiod.2013.12.002

Chen Q, Zhang D, Pan W, Ouyang Q, Li H, Urmila K, Zhao J (2015) Recent developments of green analytical techniques in analysis of tea's quality and nutrition. Trends Food Sci Technol 43(1):63-82. https://doi.org/10.1016/j.tifs.2015.01.009

Deepa MS, Shukla SR, Kelkar BU (2024) Overview of applications of near infrared (NIR) spectroscopy in wood science: recent advances and future prospects. J Indian Acad Wood Sci 1-24.

Fackler K, Schwanninger M (2012) How spectroscopy and microspectroscopy of degraded wood contribute to understand fungal wood decay. Appl Microbiol Biotechnol 96:587-599. https://doi.org/10.1007/s00253-012-4369-5

Fackler K, Schwanninger M, Gradinger C, Srebotnik E, Hinterstoisser B, Messner K (2007) Fungal decay of spruce and beech wood assessed by near-infrared spectroscopy in combination with uni-and multivariate data analysis.

Gauthier S, Bernier P, Kuuluvainen T, Shvidenko AZ, Schepaschenko DG (2015) Boreal forest health and global change. Science 349(6250):819-822. http://www.jstor.org/stable/24749186

González-Peña MM, Curling SF, Hale MD (2009) On the effect of heat on the chemical composition and dimensions of thermally-modified wood. Polym Degrad Stab 94(12):2184-2193.

Guillén Y, Machuca Á (2008) The effect of copper on the growth of wood-rotting fungi and a blue-stain fungus. World J Microbiol Biotechnol 24:31-37. https://doi.org/10.1007/s11274-007-9434-3

Hein PRG, Pakkanen HK, Dos Santos AA (2017) Challenges in the use of Near Infrared Spectroscopy for improving wood quality: A review. Forest

Syst 26(3):eR03. https://doi.org/10.5424/fs/2017263-11892

Jain P, Barber QE, Taylor SW, Whitman E, Castellanos Acuna D, Boulanger Y, Chavardès RD, Chen J, Englefield P, Flannigan M, Girardin MP, Hanes CC, Little J, Morrison K, Skakun RS, Thompson DK, Wang X, Parisien M-A (2024) Drivers and impacts of the record-breaking 2023 wildfire season in Canada. Nat Commun 15:Article 6764. https://doi.org/10.1038/s41467-024-51154-7

Kelley SS, Jellison J, Goodell B (2002) Use of NIR and pyrolysis-MBMS coupled with multivariate analysis for detecting the chemical changes associated with brown-rot biodegradation of spruce wood. FEMS Microbiology Letters, 209(1), 107-111. https://doi.org/10.1111/j.1574-6968.2002.tb11117.x

Lang C, Almeida DR, Costa FR (2017) Discrimination of taxonomic identity at species, genus and family levels using Fourier Transformed Near-Infrared Spectroscopy (FT-NIR). For Ecol Manage 406:219-227.

Lundell TK, Mäkelä MR, de Vries RP, Hildén KS (2014) Genomics, lifestyles and future prospects of wood-decay and litter-decomposing basidiomycota. Adv Bot Res 70:329-370.

Mensah RA, Jiang L, Renner JS, Xu Q (2023) Characterisation of the fire behaviour of wood: From pyrolysis to fire retardant mechanisms. J Therm Anal Calorim 148(4):1407-1422. https://doi.org/10.1007/s10973-022-11442-0

McCarthy JK, Hood IA, Kimberley MO, Didham RK, Bakys R, Fleet KR, Brownlie RK, Flint HJ, Brockerhoff EG (2012) Effects of season and region on sapstain and wood degrade following simulated storm damage in Pinus radiata plantations. For Ecol Manage 277:81–89. https://doi.org/10.1016/j.foreco.2012.04.018

Natural Resources Canada (2023). The State of Canada's Forests: Annual Report 2023. Retrieved from https://natural-resources.canada.ca/sites/nrcan/files/forest/sof2023/NRCAN_SofForest_Annual_2023_EN_accessible-vf.pdf

Natural Resources Canada (2022). Canada's softwood lumber industry. Retrieved from https://natural-resources.canada.ca/our-natural-resources/forests/industry-and-trade/canadas-softwood-lumber-industry/19601

Natural Resources Canada (2020). Economic impacts. Retrieved from https://natural-resources.canada.ca/our-natural-resources/forests/insects-disturbances/forest-pest-management/economic-impacts/13387

Natural Resources Canada (2019). Changes in temperature. Retrieved from https://www.canada.ca/en/environment-climate-change/services/climate-change/canadian-centre-climate-services/basics/trends-projections/changes-temperature.html

Oksanen J, Simpson GL, Blanchet FG, Kindt R, Legendre P, Minchin PR, O'Hara RB, Solymos P, Stevens MHH, Szoecs E, Wagner H, Barbour M, Bedward M, Bolker B, Borcard D, Carvalho G, Chirico M, De Caceres M, Durand S, Evangelista HBA, FitzJohn R, Friendly M, Furneaux B, Hannigan G, Hill MO, Lahti L, McGlinn D, Ouellette M-H, Ribeiro Cunha E, Smith T, Stier A, Ter Braak CJF, Weedon J (2024) vegan: Community ecology package (Version 2.6-6.1) [R package]. CRAN. https://CRAN.R-project.org/package=vegan

Piernik M, Woźniak M, Pinkowski G, Szentner K, Ratajczak I, Krauss A (2022) Impact of the heat treatment duration on color and selected mechanical and chemical properties of scots pine wood. Materials 15(15):5425.

Pohleven F, Humar M, Amartey S, Benedik J (2002) Tolerance of wood decay fungi to commercial copper-based wood preservatives. IRG/WP 02-30291.

Ramirez JA, Posada JM, Handa IT, Hoch G, Vohland M, Messier C, Reu B (2015) Near-infrared spectroscopy (NIRS) predicts non-structural carbohydrate concentrations in different tissue types of a broad range of tree species. Methods Ecol Evol 6(9):1018–1025.

R Core Team (2024) R: A language and environment for statistical computing. R Foundation for Statistical Computing, Vienna, Austria. https://www.R-project.org/.

Savitzky A, Golay MJ (1964) Smoothing and differentiation of data by simplified least squares procedures. Anal Chem 36(8):1627–1639.

Schmidt O (2006) Wood and tree fungi. Springer-Verlag Berlin Heidelberg.

signal developers (2023) signal: Signal processing. Retrieved from https://r-forge.r-project.org/projects/signal/

Si-Ware Systems. (2023). NeoSpectra Scanner. Retrieved April 8, 2025, from https://www.si-ware.com/neospectra-product-pages/scanner

Sundaram J, Mani S, Kandala CV, Holser RA (2015) Application of NIR reflectance spectroscopy on rapid determination of moisture content of wood pellets. Am J Anal Chem 6(12):923–932.

Schwanninger M, Rodrigues JC, Fackler K (2011) A review of band assignments in near infrared spectra of wood and wood components. J Near Infrared Spectrosc 19(5):287–308.

Tsuchikawa S, Inagaki T, Ma T (2023) Application of near-infrared spectroscopy to forest and wood products. Curr For Rep 9:401–412. https://doi.org/10.1007/s40725-023-00203-3

Tsuchikawa S, Kobori H (2015) A review of recent application of near-infrared spectroscopy to wood science and technology. J Wood Sci 61:213–220. https://doi.org/10.1007/s10086-015-1467-x

Tsuchikawa S (2007) A review of recent near-infrared research for wood and paper. Appl Spectrosc Rev 42(1):43–71.

Via BK, So CL, Eckhardt LG, Shupe TF, Groom LH, Stine M (2008) Response of near-infrared diffuse reflectance spectra to blue stain and wood age. J Near Infrared Spectrosc 16(1):71–74.

Via B, Eckhardt L, So C, Shupe T, Groom L, Stine M (2007) The response of visible/near-infrared absorbance to wood-staining fungi. Wood Fiber Sci 38(4):717–726.

Watson P, Potter S (2004) Burned wood in the pulp and paper industry: a literature review. For Chron 80(4):473–477.

Wulder MA, Hermosilla T, White JC, Coops NC (2020) Biomass status and dynamics over Canada's forests: Disentangling disturbed area from associated aboveground biomass consequences. Environ Res Lett 15.